Higher-order polarization singularitites in tailored vector beams

2016 J. Opt. 18 074012

(http://iopscience.iop.org/2040-8986/18/7/074012)

IOP Publishing Journal of Optics
J. Opt. 18 (2016) 074012 (7pp) doi:10.1088/2040-8978/18/7/074012

Higher-order polarization singularitites in tailored vector beams

E Otte, C Alpmann and C Denz

Institute of Applied Physics, University of Muenster, Corrensstr. 2/4, D-48149 Muenster, Germany

E-mail: eileen.otte@uni-muenster.de

Received 31 January 2016, revised 4 May 2016
Accepted for publication 10 May 2016
Published 8 June 2016

Abstract

Higher-order polarization singularities embedded in tailored vector beams are introduced and experimentally realized. As holographic modulation allows to define order and location of any vectorial singularity, the surrounding vector field can be dynamically shaped. We demonstrate light fields associated with flowers or spider webs due to regular and even irregular patterns of the orientation of polarization ellipses. Beyond that, not yet investigated hybrid structures are introduced that allow generating networks of flowers and webs in very close vicinity. Our results pave the way to applications of singular optics in spatially extended, optimized optical tweezing and high-resolution imaging.

Keywords: higher-order, vector beams, Poincaré beams, holographic modulation, hybrid beams, polarization singularitites, optical tweezers

1. Introduction

Tailored light fields spatially varying in amplitude and phase are well established in optics, as witnessed by a number of different applications in optical manipulation and optical trapping [1–4]. An intriguing, aspiring field of tailored light with fundamental significance is singular optics. In this, fundamental topological properties of electromagnetic waves, as singularities and dislocations in phase and polarization, are investigated [5, 6].

In spatially structured light, the distribution of phase can create dislocations in which the phase is undefined and intensity vanishes. These *scalar phase singularities* occur in the center of optical vortices [5, 7, 8], and have been investigated for already many years in singular optics [5, 9]. They can be observed naturally within speckle fields or generated by e.g. holographic techniques shaping the light field's topology [3, 4]. Beside phase singularities, *vectorial polarization singularities* have attracted growing attention within the last years [7, 10]. Apart from their natural occurrence in e.g. the blue daylight sky caused by Rayleigh scattering of sunlight in the atmosphere [7], different kinds of polarization singularities can be observed in polarization structured light fields, also known as Poincaré beams [11–13]. In these singularities either the polarization itself (V-Point), its orientation (C-Point/ C-Line) or its handedness and ellipticity (L-Point/ -Line) is undefined [6, 7, 11, 14, 15]. Due to their inherent instability resulting from their co-dimension four [16, 17], V-Points only occur in specifically tailored light fields.

Well known examples of Poincaré beams, including polarization singularities, are azimuthally and radially polarized beams or their combinations, whose properties were already investigated intensively [18]. These fields belong to the subclass of vector beams consisting of linearly polarized states, whose orientations vary spatially [11]. An inhomogeneous distribution in orientation can cause the appearance of V-Points [19] in the beam's transverse plane. In the case of radially or azimuthally polarized beams, singularities are of first order, i.e. they are characterized by the so called Poincaré–Hopf-index [20] $\eta = 1$. This index describes the winding of a vector field on a closed curve around a singularity [20].

For these beams, interesting features have been shown, as tighter focusing by radial polarization [21], which finds applications in e.g. imaging [22–25], or even complex 3D focus shaping [26–29]. This led to rising interest in vector beams with higher-order polarization singularities ($|\eta| > 1$), expecting further, extended applications. Different approaches were taken in order to generate higher-order singular vector beams [30–33], realizing structures of axial symmetric shape with on-axis singularities. However, higher-order vector beams of tailored, asymmetric shape, which are of special interest with respect to imaging applications and fundamental

research in singular optics, have not been considered. In addition to higher-order singularities, implementations may be extended by tailoring vector fields as a new degree of freedom. Moreover, many theoretical analyses [19] with respect to irregularly shaped vector beams still need to be demonstrated and examined experimentally. This is the scope of the present publication.

In this publication we introduce tailored vector beams containing singularities of higher order at chosen positions. In section 2, we elucidate our experimental system used for innovative modulation of Poincaré beams, and demonstrate the realization of first-order singularities in vector fields. Next, we present the realization of on- and off-axis higher-order singularities in flower- and spider-web-like vector beams, showing a regular distribution with respect to vectors' orientation around the V-Point singularity (section 3.1). Finally, we realize beams of fully tailored shape in sections 3.2 and 3.3. Irregularly shaped flowers and spider webs, as well as original hybrid structures of these, are introduced, revealing novel insights into the fundamentals of singular optics.

2. Singular vector beams

Singular vector fields consisting of linearly polarized states naturally include polarization singularities. The orientation of polarization states varies within the transverse plane, facilitating the occurrence of V-Points, in which the polarization is undefined and intensity vanishes. These singularities are characterized by an index depending on the surrounding light field, as it will be described below in more detail. Moreover, our modulation method and exemplary experimental realizations of first-order singular vector beams will be presented.

2.1. Dynamic polarization modulation system (DPMS)

Different methods were developed in order to generate vector beams. Some examples are active modulation by intracavity axial birefringent components [35], or the use of a radial analyzer made of birefringent [36] or dichroic materials [37], having its local polarization transmission axis aligned along the radial or the azimuthal direction. However, these methods do neither allow a variable modulation of linear states, nor an arbitrary transverse location of possible polarization singularities. Moreover, the order of singularities is also restricted in these cases.

In order to expand the methods' capabilities, different approaches were pursued [30–34], whereby we choose a single-beam holographic method for a dynamic generation of tailored polarization structured beams with higher-order polarization singularities. The modulation of the light field is performed by the DPMS, which employs a reflective phase-only spatial light modulator (SLM) as the key component in a configuration with two quarter wave plates ($QWP_{1,2}$) [38–40]. Figure 1(a) shows a sketch of the experimental configuration including the DPMS (I). After an expansion of the laser beam (wavelength $\lambda = 532$ nm) by two lenses and orienting the incoming polarization horizontally, the beam enters the DPMS.

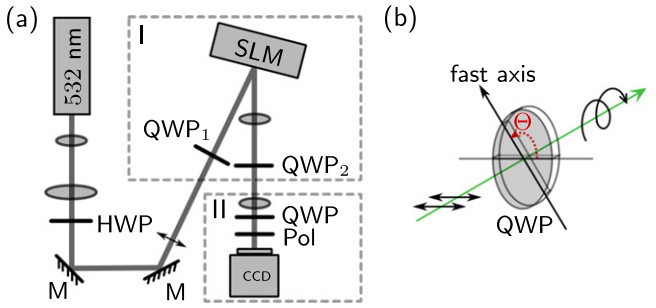

Figure 1. Dynamic polarization modulation system (DPMS): (a) Experimental configuration containing the DPMS in I and the measurement system for the spatially resolved determination of Stokes parameters in II. M: mirror, (H/ Q)WP: (half/ quarter) wave plate, SLM: phase-only spatial light modulator, Pol: polarizer, CCD: camera. (b) Definition of QWPs' angles $\Theta_{1,2}$. (see also [38]).

The angles $\Theta_{1,2}$ of the DMPS's $QWP_{1,2}$ are defined as the angles between the entering horizontal polarization and the wave plates' fast axis (see figure 1(b)). Depending on these angles and the phase shift $\Delta\Phi_{\mathbf{SLM}}$ introduced by the phase-only SLM (parallel aligned liquid crystal display), various states of polarization located on a ring on the Poincaré sphere are achievable [38]. The phase shift is caused by the fact that the SLM is only able to modulate horizontal polarization components in phase, while vertical components are only reflected. By choosing a spatially varying phase hologram $\Delta\Phi_{\mathbf{SLM}}(x, y)$, different states of polarization are realized by the DPMS in the beam's transverse plane for each pixel of the SLM, and thus, Poincaré beams are modulated [38, 39]. If $\Theta_{1,2} = \pm 45°$, linearly polarized vector beams are generated, where vectors' orientation varies spatially according to $\Delta\Phi_{\mathbf{SLM}}(x, y)$. In order to determine the output polarization spatially resolved, a rotatable quarter wave plate in combination with a fixed polarizer in front of a CCD camera is used (see figure 1(a, II)). A $2f_1$–$2f_2$-configuration images the SLM onto the camera. By measuring the pixelwise intensity on the camera as a function of the quarter wave plate's rotation angle, the Stokes parameters, and hence, the state of polarization can be obtained as described in [41].

2.2. Stokes field singularity index

To identify singularities in polarization structured light fields so called complex Stokes fields are commonly used. These are given by $\Sigma_{ij} = S_i + \mathrm{i}S_j$, in which $S_{i,j}$ with $i, j = \{1, 2, 3\}$ are the normalized Stokes parameters [42, 43]. To distinguish between different kinds of linearly polarized vector beams, and to characterize the order of an occurring polarization singularity (V-Point), the Stokes field Σ_{12} and the corresponding singularity index σ_{12} can be used [43]. In this case, the phase

$$\Phi_{12} = \arctan(S_2/S_1) \tag{1}$$

of the complex Stokes field

$$\Sigma_{12} = S_1 + \mathrm{i}S_2 = A_{12} \cdot \exp(\mathrm{i}\Phi_{12}) \tag{2}$$

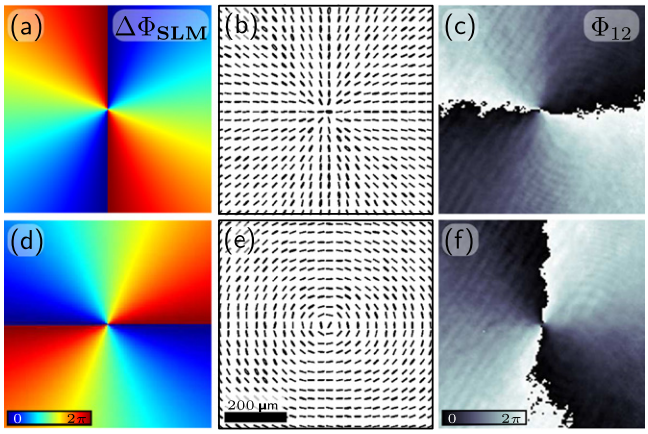

Figure 2. Modulation of positive first-order singularities in vector beams: (a), (d) show the phase holograms $\Delta\Phi_{\mathbf{SLM}}$ used for the generation of (b) radially and (e) azimuthally oriented polarization distributions ($\Theta_1 = -\Theta_2 = -45°$). The states of polarization are indicated by small polarization ellipses of every fifth camera pixel. The central first-order V-Points can be detected in the Stokes field's phase distribution in (c), (f). The singularities are characterized by the indices $\sigma_{12} = 2$ or $\eta = 1$.

with $A_{12} = \sqrt{S_1^2 + S_2^2}$ is defined by the normalized, measurable Stokes parameters S_1 and S_2. A vectorial singularity in the form of a V-Point can be detected as a singular point of undefined phase in the center of a phase vortex in Φ_{12}. Consequently, the corresponding Stokes field singularity index is given by [7, 43]

$$\sigma_{12} = \frac{1}{2\pi} \oint_C \mathbf{d}\Phi_{12} = \frac{\Delta\Phi_{12}}{2\pi}, \tag{3}$$

whereby $\Delta\Phi_{12}$ quantifies the azimuthal, counterclockwise variation of the phase Φ_{12} of the complex Stokes field around the singularity. Alternatively, the Poincaré–Hopf-index η is used, which is related to the Stokes field index by the equation $\sigma_{12} = 2\eta$ ($\eta \in \mathbb{Z}$) [43]. Thus, first-order singularities having a Poincaré–Hopf-index of $|\eta| = 1$ reveal a Stokes singularity index of $|\sigma_{12}| = 2$. Accordingly, V-Points are named higher-order singularities if they show indices $|\sigma_{12}| > 2$ or $|\eta| > 1$.

2.3. First-order vectorial singularities

First-order singularities in e.g. azimuthally or radially polarized vector beams can be directly modulated by the use of the DPMS choosing $\Theta_{1,2} = \pm 45°$. In the case at hand, the angles are set to $\Theta_1 = -\Theta_2 = -45°$, whereby different combination would be feasible, too. Figures 2(b) and (e) show the experimental results of a radially and an azimuthally oriented vector field achieved by using the phase holograms depicted in (a) and (d), respectively. Note that an additional correction pattern has been applied in order to correct errors caused by the SLM's uneven surface [39]. In (b), (e), the resulting polarization distribution in the transverse plane of the modulated beam is indicated in the form of polarization ellipses determined by Stokes parameters measurements for every fifth camera pixel. As expected for linear states of polarization of vector beams, the polarization ellipses have an ellipticity of almost zero and appear as a line. In the center of both generated beams a vectorial singularity in the form of a V-Point can be detected: The corresponding phase Φ_{12} of the Stokes field, calculated from measured parameters, shows a phase vortex with a central singular point in (c), (f). The appendant singularity index is $\sigma_{12} = +2$ ($\eta = +1$) for both modulated (positive) first-order singularities located in the radially and azimuthally polarized vector beams. As typical for V-Points, the beam's intensity solely vanishes at the singularities' origin, whereas the rest of the transverse plane shows a nearly homogeneous intensity distribution. If negative first-order singularities are desired ($\sigma_{12} = -2$ or $\eta = -1$), the sign of the modulation hologram $\Delta\Phi_{\mathbf{SLM}}$ can be inversed.

Due to the modulation technique, both beams show a spiral phase front verified by single slit diffraction [44]. In order to avoid this effect, a double-pass of the SLM enabling an additional phase correction can be used as described in [38, 39].

The modulated beams reveal a high precision regarding vectors' orientation and linearity of polarization states, facilitated by the holographic modulation system. This effect is visible in the homogeneity of the gradient of Φ_{12} in (c), (f), and in very narrow polarization ellipses in (b), (e), respectively.

3. Higher-order singularities

As already indicated, besides the generation of first-order singularities our system is also able to modulate higher-order singularities. Especially for this purpose, another characteristic of the DPMS is of particular interest: For $\Theta_1 = \Theta_2 = -45°$, the phase hologram $\Delta\Phi_{\mathbf{SLM}}$ is equal to the Stokes field's phase Φ_{12} of the modulated transverse vector field. This means, we are able to directly modulate the Stokes field's phase by the choice of the hologram and, consequently, predefine the number, order and position of the singularities within the beam's transverse plane.

In the following, we present the realization of positively and negatively indexed singularities, showing experimental results regarding V-Points of higher order and chosen position.

3.1. Flowers and spider webs

Vector fields with isolated higher-order singularities can be distinguished according to their V-Point's index [19]: vector fields with singularities of positive index $\sigma_{12} \geqslant 2$ are oriented in forms similar to flowers; whereas, if the singularity is negatively indexed with $\sigma_{12} \leqslant -2$, the vector beam reveals the shape of a spider web. The number of flower petals and spider web sectors is directly related to the singularity index by $\sigma_{12} - 2$ and $|\sigma_{12}| + 2$, respectively [43].

Figure 3 depicts examples of different kinds of vector beams with higher-order singularity. By applying holograms $\Delta\Phi_{\mathbf{SLM}}$ resembling phase vortices of higher topological charges l (defined by the change of phase around the central

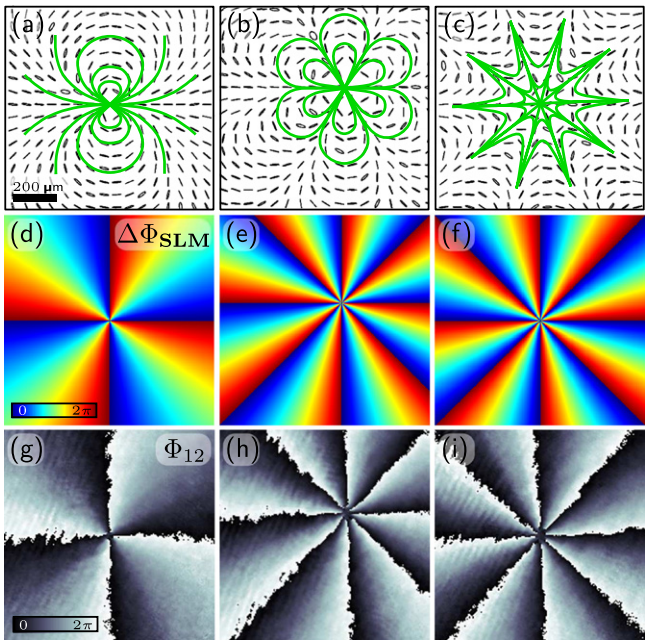

Figure 3. Higher-order V-Points in vectorial flowers and spider webs: (a)–(c) depict the transverse polarization distribution experimentally realized by the phase holograms $\Delta\Phi_{\mathbf{SLM}}$ in (d)–(f), respectively. $\Delta\Phi_{\mathbf{SLM}}$ in (d)–(f) equals the corresponding measured phase Φ_{12} of the complex Stokes field in (g)–(i), due to the choice of $\Theta_{1,2} = -45°$. Φ_{12} reveals the indices $\sigma_{12} = +4,\ +8$ and -8 for the V-Points located in polarization distributions resembling (a) a two-fold flower (spider), (b) a six-fold flower, and (c) a ten-fold web as indicated by drawn flow lines (green).

phase singularity divided by 2π), we gain vector fields with higher-indexed polarization singularities. According to the vortices' sign, the vector beams are shaped as flowers or webs, due to the fact that the hologram $\Delta\Phi_{\mathbf{SLM}}$ and its topological charge l are equal to the Stokes fields phase Φ_{12} and the vectorial singularity's index σ_{12}, respectively. The V-Points' spatial position is defined by the position of the phase singularity in the hologram $\Delta\Phi_{\mathbf{SLM}}$.

Figure 3(a)–(c) shows the measured transverse polarization distributions (polarization ellipse of every tenth camera pixel) achieved from the corresponding phase holograms shown in (d)–(f). Additionally, the phase Φ_{12} of the complex Stokes field calculated according to measured Stokes parameters is depicted in (g)–(i). The comparison of phase hologram $\Delta\Phi_{\mathbf{SLM}}$ to phase Φ_{12} reveals their similarity. We obtain vectorial singularities indexed by $\sigma_{12} = l = +4,\ +8$ and -8 for the fields in (a)–(c). As a result, the corresponding vector fields have the shape of a $(\sigma_{12} - 2 =)$ two-fold flower, resembling a spider, a six-fold flower and a $(|\sigma_{12}| + 2 =)$ ten-fold spider web. These shapes are indicated by green flow lines in (a)–(c). In (a) and (c) the singularity is located in the center, while in (b) it is shifted off-axis to the upper right of the beam's transverse plane.

A key point to emphasize is the precise, regular realization of these vector fields with respect to their shape. The orientation of the polarization states surrounding a singularity, which depicts the symmetry point, forms petals or sectors of

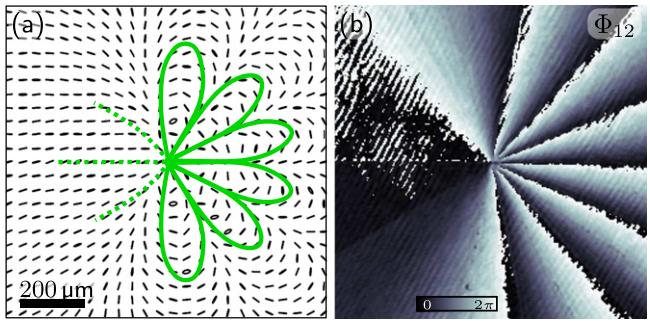

Figure 4. Tailored vectorial flower: (a) shows the measured polarization distribution superimposed by green flow lines, (b) the corresponding phase Φ_{12} of the complex Stokes field (for $\Theta_{1,2} = -45°$). The central V-Point has an index of $\sigma_{12} = 8$, thus, six petals can be observed.

the same size and shape in the regarded transverse field. This regular shape is identifiable in a transversely homogeneous phase gradient of Φ_{12}.

3.2. V-Points in tailored, irregular vector fields

Beside the generation of vector beams with a regular distribution with respect to the orientation of polarization states, we are also able to modulate irregularly shaped vector fields containing higher-order vectorial singularities. For this purpose, the QWPs of the DPMS are again set to $\Theta_{1,2} = -45°$ in order to modulate the Stokes field's phase Φ_{12} directly. By choosing phase holograms $\Delta\Phi_{\mathbf{SLM}}$, which resemble an irregular vortex including a phase singularity, the modulation of the light field results in an also irregularly shaped vector field. It is found that the phase vortex' topological charge still determines the V-Point's order ($l = \sigma_{12}$), as already described for regular structures. This direct relation between the employed modulation hologram and the resulting vector field is a distinct advantage of our method that allows for the generation of arbitrary irregularly shaped vector beams, in contrast to other previous works [34].

An example of tailored vector beams with higher-order V-Points is shown in figure 4: (a) demonstrates the experimental results of a deformed flower with a vectorial singularity of index $\sigma_{12} = 8$, superimposed by drawn flow lines. In this case, the higher-order V-Point is chosen to be located in the center of the transverse field. The flow lines of the vector field reveal petals on the right-hand side, while on the left-hand side the flow lines do not form petals by closed loops. In total, $\sigma_{12} - 2 = 6$ petals can be observed, as theoretically expected [43]. This tailored vector beam is no longer regularly shaped and point symmetric with respect to its V-Point, which is emphasized by the spatial inhomogeneous gradient of the Stokes field's phase Φ_{12} illustrated in (b). However, the beam has been precisely generated, following a predefined, irregular shape.

3.3. Generation of hybrid structures

Next, we introduce another, not yet investigated kind of vector field: hybrid structures of flowers and webs. These

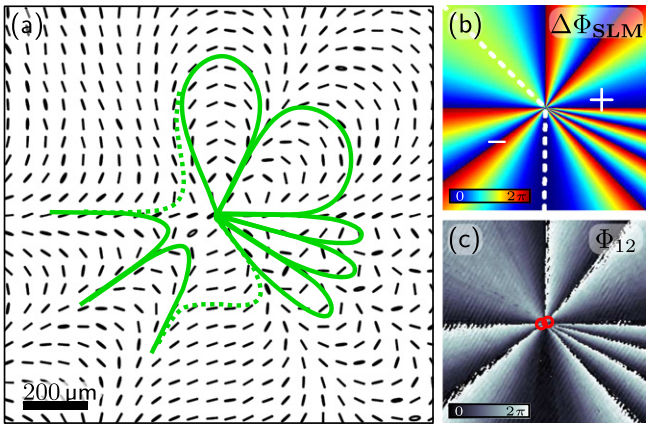

Figure 5. Hybrid vector field: (a) demonstrates an experimentally generated hybrid structure of a flower and a web as emphasized by green flow lines ($\Theta_{1,2} = -45°$). Therefore, the used phase hologram $\Delta\Phi_{\mathbf{SLM}}$ in (b) reveals areas of azimuthally positively and negatively changing phase (separated by white dotted line). The corresponding measured phase Φ_{12} of the complex Stokes field is depicted in (c), where two very close singularities (red circles) can be observed.

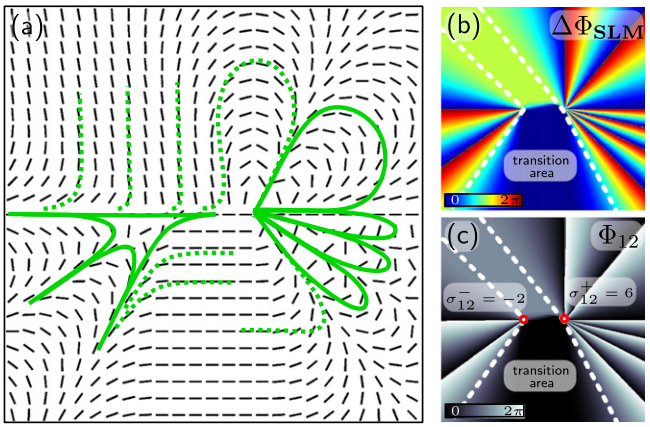

Figure 6. Increased distance of singularities: (a) shows the simulation of a joint vector field consisting of an irregularly shaped flower and web as close neighbors (see green flow lines). The vector field is calculated according to the modulation hologram $\Delta\Phi_{\mathbf{SLM}}$ in (b) ($\Theta_{1,2} = -45°$), containing areas of positive and negative gradients and a transition area between these (white dotted lines). In (c), the phase Φ_{12} of the complex Stokes field indicates two singularities (red circles) with an index of $\sigma_{12}^{-} = -2$ and $\sigma_{12}^{+} = 6$ at the areas' borderlines.

vector beams contain flower petals as well as spider web sectors and, thus, include characteristics of both field structures. The investigation of polarization singularities' occurrence, characterization and stability within these fields may open new insights into fundamentals of singular optics.

The DPMS facilitates the tailored modulation and, thereby, the analysis of hybrid structures. For the realization, modulation holograms, which show phase gradients azimuthally alternating in sign, are designed. This causes the generation of flower- and web-type vector field areas due to the direct relation between $\Delta\Phi_{\mathbf{SLM}}$ and Φ_{12} (for $\Theta_{1,2} = -45°$).

An example for such structures is illustrated in figure 5. The measured polarization distribution is illustrated in (a) with a superimposed sketch of the flow line structure, whereby in (b) the original phase hologram $\Delta\Phi_{\mathbf{SLM}}$ is shown. The corresponding Stokes field's phase Φ_{12} with transverse inhomogeneous distribution of its gradient is depicted in (c).

The modulation hologram $\Delta\Phi_{\mathbf{SLM}}$ and, thus, the phase Φ_{12} can be divided into two areas of positive and negative phase gradients, as indicated by the dotted lines in (b). To each of these areas of opposed sign belongs a characteristic type of vector field. This means that flower petals are supposed to be located in direct neighborhood to web sectors. By this, a hybrid structure of flower and web is formed as visible in the sketch of flow lines in (a).

Five petals of a flower and two sectors of a web can be observed connected by a transition area. This leads to the assumption of the existence of two closely-located asymmetric polarization singularities of opposite sign, as indicated by red circles in (c). Typically, singularities are characterized by the singularity index σ_{12} (or η), which is calculated depending on the corresponding phase Φ_{12} of the complex Stokes field (see equation (3)), and connected to the shape of the surrounding vector field [43]. In the case at hand, this characterization meets problems due to the singularities' close vicinity. Moreover, the expected indices considering the number of petals and web sector do not fit the phase distribution of Φ_{12}. From this arises the question whether it is possible to determine a singularity index for each singularity, or if an overall index for the whole hybrid structure needs to be defined.

In singular optics it is known that each blossom of flowers located in a joint vector field preserves its singularity index, unless these are not located in too close vicinity [19]. This is confirmed by the case of the shown hybrid structure. Consequently, we choose to define an overall singularity index $\sigma_{12}^{\mathbf{tot}}$ for the whole vector field. The shown hybrid structure reveals a total index of $\sigma_{12}^{\mathbf{tot}} = 4$, given by the change of phase $\Delta\Phi_{12}$ around both singularities divided by 2π.

If the distance between adjacent singularities in a joint vector field is increased, a characterization of each individual singularity by a corresponding singularity index is enabled. Moreover, the relation between number of petals or sectors and given index is recovered in this case. This is visualized by the simulation in figure 6.

By the hologram $\Delta\Phi_{\mathbf{SLM}}$ shown in (b), a joint vector field of an irregularly shaped flower and web is realized. The corresponding polarization distribution, calculated for $\Theta_{1,2} = -45°$, is depicted in (a). As illustrated by the green flow lines, the structure is composed of a deformed four-fold spider web and four-fold flower (continuous lines). In (c), the corresponding phase Φ_{12} of the complex Stokes field reveals an area of negative gradient (left), of positive gradient (right), and a transition area between these (middle) separated by white dotted lines. At the borderlines, two singularities can be detected and characterized by individual indices $\sigma_{12}^{-} = -2$ and $\sigma_{12}^{+} = 6$. These indices fit the number of sectors ($|\sigma_{12}^{-}| + 2$) and petals ($\sigma_{12}^{+} - 2$) of the deformed web and

flower represented in (a) [19]. The vector field's overall index, given by $\sigma_{12}^{\mathbf{tot}} = \sigma_{12}^{-} + \sigma_{12}^{+} = 4$, is equal to the overall index of the former hybrid structure in figure 5. However, the characterization of singularities by individual indices is only enabled in the case of increased distance between V-Points illustrated in figure 6, whereas in figure 5 this characterization is beyond the system's resolution.

As a consequence, hybrid structures facilitate the experimental analysis of singularities in close neighborhood regarding their effect e.g. on the surrounding vector field and indices, but also propagation behavior and stability, leading to further, novel insights into singular optics.

4. Conclusion

We demonstrated the modulation of tailored vector beams of regular, as well as of irregular and hybrid shape, containing first- or higher-order polarization singularities at chosen positions. These fields may extend known applications of vector beams, paving the way to e.g. neoteric information encoding, or tailored vector fields for imaging or optical tweezing. Furthermore, they contribute essentially to the fundamental research in the field of singular optics. The beams were realized by the DPMS using specified phase holograms $\Delta\Phi_{\mathbf{SLM}}$ directly connected to the phase Φ_{12} of the complex Stokes field.

By the choice of holograms resembling phase vortices and showing a transversely homogeneous distribution with respect to its phase gradient, regularly shaped flowers and spider webs containing higher-order singularities at defined positions were generated. Moreover, tailored, irregularly shaped vector fields were formed by inhomogeneously distributed phase gradients within the vortex hologram $\Delta\Phi_{\mathbf{SLM}}$ of higher topological charge l. According to the singularity index σ_{12} $(= l)$, different numbers of petal or web sectors can be observed.

Additionally, not yet investigated hybrid structures of flowers and webs were introduced, generated and analyzed. The choice of a polarization modulation hologram, which displays a transversely inhomogeneous phase gradient, azimuthally alternating in sign, resulted in a vector field composed of flower- and spider-web-like areas. Such hybrid structures show characteristics matching former theoretical analyses [19]. Further, novel, intriguing insights into fundamentals of singular optics can be obtained by the experimental analysis of hybrid structures and their singularities crowded closely together.

Acknowledgments

The authors thank the German Research Foundation (DFG) for financial support in the frame of the German-Chinese transregional research project TRR61, University of Muenster, Germany.

References

[1] Andrews D L 2011 *Structured Light and its Applications: An Introduction to Phase-Structured Beams and Nanoscale Optical Forces* (Burlington: Academic–Elsevier)
[2] Dholakia K and Čižmár T 2011 *Nat. Photon.* **5** 335–42
[3] Woerdemann M, Alpmann C, Esseling M and Denz C 2013 *Laser Photon. Rev.* **7** 839–54
[4] Alpmann C, Schöler C and Denz C 2015 *Appl. Phys. Lett.* **106** 241102
[5] Soskin M S and Vasnetsov M V 2001 *Singular Optics* (*Progress in Optics* vol 42) ed E Wolf (Amsterdam: Elsevier) pp 219–76 ch 4
[6] Kurzynowski P, Woźniak W A and Borwińska M 2010 *J. Opt.* **12** 035406
[7] Dennis M R, O'Holleran K and Padgett M J 2009 *Singular Optics: Optical Vortices and Polarization Singularities* (*Progress in Optics* vol 53) ed E Wolf (Amsterdam: Elsevier) pp 293–363 ch 5
[8] Denisenko V G, Minovich A, Desyatnikov A S, Krolikowski W, Soskin M S and Kivshar Y S 2008 *Opt. Lett.* **33** 89–91
[9] Nye J F and Berry M V 1974 *Proc. R. Soc.* A **336** 165–90
[10] Nye J F and Hajnal J V 1987 *Proc. R. Soc.* A **409** 21–36
[11] Galvez E J 2015 *Light Beams with Spatially Variable Polarization* (*Photonics, Fundamentals of Photonics and Physics* vol 1) ed D L Andrews (Hoboken: Wiley) pp 61–76 ch 3
[12] Brown T G 2011 *Unconventional Polarization States: Beam Propagation, Focusing, and Imaging* (*Progress in Optics* vol 56) ed E Wolf (Amsterdam: Elsevier) pp 81–129 ch 2
[13] Beckley A M, Brown T G and Alonso M A 2010 *Opt. Express* **18** 10777–85
[14] Freund I 2004 *Opt. Commun.* **242** 65–78
[15] Freund I 2012 *Opt. Lett.* **37** 2223–5
[16] Schoonover R W and Visser T D 2006 *Opt. Express* **14** 5733–45
[17] Vyas S, Kozawa Y and Sato S 2013 *Opt. Express* **21** 8972–86
[18] Zhan Q 2009 *Adv. Opt. Photon* **1** 1–57
[19] Freund I 2001 *Opt. Commun.* **199** 47–63
[20] Strogatz S H 2001 *Nonlinear Dynamics and Chaos: with Applications to Physics, Biology, Chemistry, and Engineering* (Boulder, CO: Westview Press)
[21] Dorn R, Quabis S and Leuchs G 2003 *Phys. Rev. Lett.* **91** 233901
[22] Biss D P and Brown T G 2003 *Opt. Lett.* **28** 923–5
[23] Carrasco S, Saleh B E A, Teich M C and Fourkas J T 2006 *J. Opt. Soc. Am.* B **23** 2134–41
[24] Biss D P, Youngworth K S and Brown T G 2006 *Appl. Opt.* **45** 470–9
[25] Bokor N and Davidson N 2004 *Opt. Lett.* **29** 1968–70
[26] Zhan Q and Leger J 2002 *Opt. Express* **10** 324–31
[27] Chen W and Zhan Q 2006 *Opt. Commun.* **265** 411–7
[28] Bokor N and Davidson N 2006 *Opt. Lett.* **31** 149–51
[29] Wang H, Shi L, Lukyanchuk B, Sheppard C and Chong C T 2008 *Nat. Photon.* **2** 501–5
[30] Neil M A A, Massoumian F, Juškaitis R and Wilson T 2002 *Opt. Lett.* **27** 1929–31
[31] Maurer C, Jesacher A, Fürhapter S, Bernet S and Ritsch-Marte M 2007 *New J. Phys.* **9** 78
[32] Cardano F, Karimi E, Slussarenko S, Murracci L, de Lisio C and Santamoto E 2012 *Appl. Opt.* **51** C1–6
[33] Galvez E J, Khadka S, Schubert W H and Nomoto S 2012 *Appl. Opt.* **51** 2925–34
[34] Moreno I, Davis J A, Cottrell D M and Donoso R 2014 *Appl. Opt.* **53** 5493–501
[35] Pohl D 1972 *Appl. Phys. Lett.* **20** 266–7

[36] Zhan Q and Leger J R 2002 *Appl. Opt.* **41** 4630–7
[37] Zhan Q and Leger J R 2002 *Opt. Commun.* **213** 241–5
[38] Alpmann C, Schlickriede C, Otte E and Denz C 2016 Dynamic modulation of Poincaré beams (submitted)
[39] Otte E, Schlickriede C, Alpmann C and Denz C 2015 Complex light fields enter a new dimension: holographic modulation of polarization in addition to amplitude and phase *Proc. SPIE* **9379** 937908
[40] Han W, Yang J, Cheng W and Zhan Q 2013 *Opt. Express* **21** 20692–706
[41] Schaefer B, Collett E, Smyth R, Barrett D and Fraher B 2007 *Am. J. Phys.* **75** 163–8
[42] Freund I 2001 *Opt. Lett.* **26** 1996–8
[43] Freund I 2002 *Opt. Commun.* **201** 251–70
[44] Ghai D P, Senthilkumaran P and Sirohi R S 2009 *Opt. Lasers Eng.* **47** 123–6